JMR Abstracts

Abstracts for July 1995 Journal of Materials Research   *Volume 10, Number 7*

TABLE OF CONTENTS

Low Temperature/Low Pressure Hydrothermal Synthesis
of Barium Titanate: Powder and Heteroepitaxial Thin Films
A.T. Chien, J.S. Speck, F.F. Lange, A.C. Daykin, C.G. Levi

Microstructures and Interdiffusions of Pt/Ti Electrodes
with Respect to Annealing in the Oxygen Ambient
K.H. Park, C.Y. Kim, Y.W. Jeong, H.J. Kwon, K.Y. Kim, J.S. Lee, S.T. Kim

Chemical Analyses of Stains Formed on Co-Nb-Zr MIG Heads Sliding
Against Oxide and Metal Particle Magnetic Tapes
B.K. Gupta, B. Bhushan, Y. Zhou, N. Winograd, K. Krishnan

Composites of Polypyrrole and Carbon Black. III. Chemical Synthesis
and Characterization
W.A. Wampler, K. Rajeshwar, R.G. Pethe, R.C. Hyer, S.C. Sharma

Removal of Residual Chromium from Aluminum Oxide
by Containerless Liquid-Phase Processing
A. Biswas, J.K.R. Weber, P.C. Nordine

A Micromechanistic Model of the Combined Combustion Synthesis-
Densification Process
Y. Zhang, G.C. Stangle

Sintering-Viscosity Relation for Mixed-Alkali Glass Powder Compacts
K-D. Kim

ABSTRACTS

COMMUNICATIONS

Preparation of Acicular Particles of Alpha-Alumina
T. Iga, Y. Murase
(National Industrial Research Institute of Nagoya)
    Aluminum ammonium sulfate solution (0.1 mol/l) and ammonium hydrogencarbonate solution (1.2 mol/l) were allowed to react at room temperature. The precipitates formed were kept with the mother liquor in a closed vessel and aged at 100°C. Acicular shaped crystalline particles of $Al(NH_4)CO_3(OH)_2$, (AACH), were obtained after the elongated aging period. Acicular α-alumina particles were obtained, through the thermal decomposition at 1300°C, out of the AACH particles which were previously treated with a small amount of tetraethoxysilane (about 1.6 wt.% of SiO_2).
Order No.: JA507-001   © **1995 MRS**

X-ray Diffraction and High-Resolution Transmission Electron Microscopy Study on A-Site Ordering of Lanthanum-Modified Lead Zirconate Titanate Relaxor
F. Fang, X. Zhang
(Tsinghua University)
    The ordering behavior of La-modified lead zirconate titanate relaxor (PLZT 9/65/35) was investigated by using x-ray diffractometer and high-resolution transmission electron microscopy (HRTEM). It was shown that {h+1/2,k+1/2,0}-type superlattice exists both in x-ray diffraction (XRD) pattern and selected electron diffraction (SAD) images. High-resolution electron micrographs further demonstrated the existence of the superlattice and exposed the ordered and disordered regions in the lattice level. A model referring A-site body-centered pseudo-cubic superstructure was proposed.
Order No.: JA507-002   © **1995 MRS**

Electron Emission from Chemical Vapor Deposition Diamond and Amorphous Carbon Films Observed with a Simple Field Emission Device
Z. Feng, I.G. Brown, J.W. Ager III
(Lawrence Berkeley Laboratory/University of California-Berkeley)
    Electron emission from chemical vapor deposition (CVD) diamond and amorphous carbon (a-C) films was observed with a simple field emission device (FED). Both diamond and a-C films were prepared with microwave plasma enhanced CVD techniques. Electron emission in the field strength range +10 to -10 MV m^{-1} was studied, and the field emission source was confirmed by a diode characteristic of the I-V curve, a straight line in the Fowler-Nordheim (F-N) plot, and direct observation of light emission from a fluorescent screen. The turn-on field strength was ~5 MV m^{-1}, which was similar for both kinds of carbon films. The highest current density for diamond films, observed at a field strength of 10 MV m^{-1}, was ~15 μA cm^{-2}. Diamond films yielded a higher emission current than a-C films. The reasons for the observed field emission are discussed.
Order No.: JA507-003   © **1995 MRS**

Molecular Dynamics Simulations of Grain Boundary Diffusion in Al Using Embedded Atom Method Potentials
C-L. Liu*, S.J. Plimpton[+]
*(*Oak Ridge National Laboratory, [+]Sandia National Laboratories)*
    Molecular dynamics simulations of diffusion in a $\Sigma5(310)[001]$ Al tilt grain boundary were performed using for the first time three different potentials based on the embedded atom method (EAM). The EAM potentials which produce more accurate melting temperatures also yield activation energies in better agreement with experimental data. Compared to pair potentials, the EAM potentials also give more accurate results.
Order No.: JA507-004   © **1995 MRS**

ARTICLES

Y123 Single Crystal Growth by the Pulling Method with Crystal Rotation Effect Control
Y. Namikawa, M. Egami, Y. Yamada, Y. Shiohara
(Superconductivity Research Laboratory-ISTEC)
    $YBa_2Cu_3O_{7-x}$ (Y123) single crystals have been grown by the modified pulling method (Solute Rich Liquid Crystal Pulling method; SRL-CP method). For further superconductor device application, it is important to establish a technique which enables us to produce larger Y123 single crystals consistently. We have investigated the relationship between the crystal size, the crystal rotation rate, the flow pattern in the melt and the temperature at the crystal growth interface experimentally. Increase of the crystal diameter and/or the crystal rotation rate increased the strength of the forced convection in the melt, and as a result, the temperature at the crystal growth interface increased. This resulted in a reduction of the crystal growth rate. On the other hand, the forced convection should be kept high enough to prevent floating particles attaching to the growing crystal. Therefore, in order to grow a larger single crystal it was necessary to control the crystal rotation rate according to the change of the crystal diameter with time. We succeeded in crystal pulling along the c-axis of a relatively large Y123 single crystal which was 17 mm x 17 mm and 8 mm in length.
Order No.: JA507-005   © **1995 MRS**

Growth Rate Estimation of YBa$_2$Cu$_3$O$_x$ Single Crystal Grown by Crystal Pulling

Y. Yamada, C. Krauns, M. Nakamura, M. Tagami, Y. Shiohara
(Superconductivity Research Laboratory-ISTEC)

We have estimated the growth rate of the YBa$_2$Cu$_3$O$_x$ crystal grown from the solution by crystal pulling, in terms of solute diffusion in the liquid with convection. The maximum growth rate deduced from the solute diffusion rate is roughly estimated to be about 1 order larger than the typical measured value. This implies that the driving force for the surface reaction is significantly larger when compared to the total driving force for the growth of YBa$_2$Cu$_3$O$_x$ crystal in our method.

Order No.: JA507-006   **© 1995 MRS**

Non-Uniform Distribution of Second Phase Particles in Melt-Textured Y-Ba-Cu-O Oxide with Metal Oxide (CeO$_2$, SnO$_2$ and ZrO$_2$) Addition

C-J. Kim*, K-B. Kim*, C-W. Hong*, H-Y. Lee[+]
*(*Superconductivity Research Laboratory-Korea Atomic Energy Research Institute, [+]Sungwha University)*

Segregation of second phase particles within Y$_1$Ba$_2$Cu$_3$O$_{7-y}$ domain was investigated in melt-textured Y-Ba-Cu-O with metal oxide (CeO$_2$, SnO$_2$ and ZrO$_2$) addition. It is found that coarse particles (Y$_2$Ba$_1$Cu$_1$O$_5$) are trapped with a special pattern in the interior of Y$_1$Ba$_2$Cu$_3$O$_{7-y}$ domain while fine BaCeO$_3$ and BaSnO$_3$ particles are present within the remnant liquid-phase region. During the growth of Y$_1$Ba$_2$Cu$_3$O$_{7-y}$ domain, fine particles appear to be pushed out of the advancing Y$_1$Ba$_2$Cu$_3$O$_{7-y}$/liquid interface toward the liquid phase. The particle segregation which occurs during peritectic growth of Y$_1$Ba$_2$Cu$_3$O$_{7-y}$ domain was explained in terms of the Uhlmann-Chalmers-Jackson's theory based on the particles interaction at solid/liquid interface.

Order No.: JA507-007   **© 1995 MRS**

Control of Y$_2$BaCuO$_5$ Size and Morphology in Melt-Processed YBa$_2$Cu$_3$O$_{7-\delta}$ Superconductor

N. Sakai, S.I. Yoo, M. Murakami
(Superconductivity Research Laboratory-ISTEC)

The important factors governing the size and the morphology of Y$_2$BaCuO$_5$ (Y211) at 1100°C in air were investigated for three different starting materials having the same nominal composition of Y: Ba: Cu = 1.8 : 2.4 : 3.4 : Y$_2$BaCuO$_5$-BaCuO$_2$-CuO-Pt, Y$_2$O$_3$-BaCu$_2$O-CuO-Pt, and melt-quenched materials from 1400°C in a Pt crucible. With various amounts of Pt doping, the heating rate and the holding time were employed as the processing parameters. With an aid of Pt doping as the effective growth inhibitor, fine round Y211 grains could be obtained by simply employing a refined round Y211 precursor and a rapid heating. There were several important factors for obtaining fine acicular (or needle-like) Y211 grains as follows: (1) The Pt dopants dissolved in the liquid phase should act as the effective heterogeneous nucleation sites; (2) Y211 grains should grow into the acicular shapes before the system reaches an equilibrium amount of Y211 in the liquid (i.e., reaction-controlled); and (3) A large amount of the liquid phase should be supplied instantly at the partial melt stage with a rapid heating.

Order No.: JA507-008   **© 1995 MRS**

Oxygen Diffusion through Dielectrics: A Critical Parameter in High Critical Temperature Superconducting Multilayer Technology

S.C. Tidrow, W.D. Wilber, A. Tauber, S.N. Schauer, D.W. Eckart, R.D. Finnegan, R.L. Pfeffer
(U.S. Army Research Laboratory-Electronics and Power Sources Directorate)

We have studied the relative diffusion rates of oxygen through dielectric/buffer layers used in high critical temperature superconducting (HTSC) multilayer structures. Epitaxial bilayer films of dielectric (CeO$_2$, LaGaO$_3$, NdGaO$_3$, LaAlO$_3$, MgO, SrTiO$_3$, LaLiTi$_2$O$_6$ or LaNaTi$_2$O$_6$) on YBa$_2$Cu$_3$O$_{7-\delta}$ (YBCO) have been deposited onto (001) oriented single crystal MgO substrates using pulsed laser deposition. These bilayers have been investigated for oxygen diffusion over the temperature range 350 to 650°C by post deposition annealing the films for 20 min in 0.5 atm of ^{18}O enriched molecular oxygen gas. Secondary ion mass spectroscopy was used to depth profile the relative concentration of ^{18}O to ^{16}O in each bilayer. Compared to YBCO, the dielectrics MgO, SrTiO$_3$, LaLiTi$_2$O$_6$ and LaNaTi$_2$O$_6$ are relatively slow diffusers, while CeO$_2$, LaGaO$_3$, NdGaO$_3$ and LaAlO$_3$ are relatively fast diffusers.

Order No.: JA507-009   **© 1995 MRS**

Crystallization and In-Plane Alignment Behavior of YBa$_2$Cu$_3$O$_{7-y}$ Films on MgO(001) Prepared by Dipping-Pyrolysis Process

T. Manabe, I. Yamaguchi, S. Nakamura, W. Kondo, T. Kumagai, S. Mizuta
(National Institute of Materials and Chemical Research)

The effects of annealing temperature and oxygen partial pressure [p(O$_2$)] were investigated on the crystallization and orientation of YBa$_2$Cu$_3$O$_{7-y}$ (YBCO) films on MgO(001) prepared by dipping-pyrolysis process. The c-axis oriented films without in-plane alignment were prepared by annealing in the YBCO-unstable region, i.e., at low initial p(O$_2$) of 10^{-4}–10^{-3} atm and 950°C followed by O$_2$ treatment, through intermediate Y$_2$BaCuO$_5$ and liquid phase. In-plane aligned c- or c/a-axis films were prepared by similar heat treatment with initial p(O$_2$) of 10^{-4} atm and 925–900°C through a mixture of BaCu$_2$O$_2$ and YBa$_3$Cu$_2$O$_{6+x}$. In contrast, non-oriented YBCO films were obtained by annealing at higher initial p(O$_2$)'s and lower temperatures, i.e., by direct reaction among Y$_2$O$_3$, BaCO$_3$ and CuO.

Order No.: JA507-010   **© 1995 MRS**

Gas-Phase Particle Size Distributions and Lead Loss During Spray Pyrolysis of (Bi,Pb)-Sr-Ca-Cu-O

A.S. Gurav*, T.T. Kodas*, J. Joutsensaari[+], E.I. Kauppinen[+], R. Zilliacus[+]
*(*University of New Mexico, [+]Technical Research Center of Finland-VTT)*

Gas-phase particle size distributions and lead loss were measured during formation of (Bi,Pb)-Sr-Ca-Cu-O and pure PbO particles by spray pyrolysis at different temperatures. A differential mobility analyzer (DMA) in conjunction with a condensation particle counter (CPC) was used to monitor the gas-phase particle size distributions, and a Berner-type low-pressure impactor was used to obtain mass size distributions and size-classified samples for chemical analysis. For (Bi,Pb)-Sr-Ca-Cu-O, as the processing temperature was raised from 200 to 700°C, the number average particle size decreased due to metal nitrate decomposition, intraparticle reactions forming mixed-metal oxides and particle densification. The geometric number mean particle diameter was 0.12 µm at 200°C and reduced to 0.08 and 0.07 µm, respectively, at 700 and 900°C. When the reactor temperature was raised from 700 and 800°C to 900°C, a large number (~10^7 #/cm^3) of new ultrafine particles were formed from PbO vapor released from the particles and the reactor walls. Particles made at temperatures up to 700°C maintained their initial stoichiometry over the whole range of particle sizes monitored, however, those made at 800°C and above were heavily depleted in lead in the size range 0.5-5.0 µm. The evaporative losses of lead oxide from (Bi,Pb)-Sr-Ca-Cu-O particles were compared with the losses from PbO particles to gain insight into the pathways involved in lead loss and the role of intraparticle processes in controlling it.

Order No.: JA507-011   **© 1995 MRS**

A Study of Temperature and Pressure Induced Structural and Electronic Changes in SbCl$_5$ Intercalated Graphite: Part IV. The Basal Plane Resistivity

O.E. Andersson*, B. Sundqvist*, E. McRae[+], M. Lelaurain[+], J.F. Marêché[+]
*(*University of Umeå, [+]Université de Nancy I)*

Using an inductive technique, we have measured the in-plane resistivity ρ_a of stages 2,4,5 and 8 SbCl$_5$-GICs versus temperature T and pressure p in the ranges 130–300 K and 0–0.85 GPa. The room temperature values of ρ_a range from 4.0 µΩcm for the stage 5 sample to 7.7 µΩcm for the stage 8 sample. At all pressures, ρ_a shows a

metallic temperature dependence $\rho_a \sim T^\alpha$, with $1 \leq \alpha \leq 2$, but in contrast to the c-axis resistivity ρ_c, it depends only very weakly on pressure and/or intercalate structural order. We show that the behavior observed is consistent with a band conduction model.
Order No.: JA507-012   © 1995 MRS

Silver-Palladium Alloy Particle Production by Spray Pyrolysis
T.C. Pluym*, T.T. Kodas*, L-M. Wang+, H.D. Glicksman+
*(*University of New Mexico, +DuPont Company)*

Spray pyrolysis was used to produce submicron Ag-Pd metal alloy particles for applications in electronic component fabrication. The particles were prepared in nitrogen carrier gas from metal nitrate precursor solutions with various compositions. The Ag-Pd alloy was the predominant phase for reactor temperatures of 700°C and above for all compositions. The 70–30 Ag-Pd particles were fully dense at 700°C, but an increased reaction temperature was necessary to produce dense particles at higher Pd to Ag ratios. The extent of palladium oxidation was suppressed with increased amounts of Ag. Single-crystal particles could be produced at sufficiently high temperatures. These results show that particle phase composition, size, oxidation behavior and morphology can be controlled by the Ag-Pd ratio in the precursor solution and by the reaction temperature.
Order No.: JA507-013   © 1995 MRS

Aspects of the Shi-Seinfeld-Okuyama Theory of Transient Nucleation
G. Sundar, J.J. Hoyt
(Washington State University)

The analytic solution to the time-dependent nucleation problem by Shi-Seinfeld-Okuyama (SSO) (Phy. Rev. A, **41**, 2101, 1990) is reviewed. The singular perturbation solution employed by SSO is extended to examine the effect of initial quench position on the incubation time. Two cases are discussed; the first investigates the role of excess vacancies from the high temperature quench on the transient kinetics. The second case examines the change in the incubation time due to the effects of a preexisting subcritical cluster size distribution which forms during the high temperature anneal.
Order No.: JA507-014   © 1995 MRS

Hydrogen Desorption Properties and Electrode Performances of Ti-Zr-Ni-V-Mn Alloy
H.W. Yang*, W.S. Lee*, Y.Y. Wang*, C.C. Wan*, T.W. Cheng+, K.H. Liang+
*(*National Tsing-Hua University, +Pao-Chang Company)*

The measurements of desorption pressure-composition-temperature (P-C-T) of $Ti_xZr_{1-x}Ni_yV_{2-y}$ ($0 \leq x \leq 1$, $0 \leq y \leq 2$) alloy have been investigated by means of 3^2 factorial design method. The response surface function of hydrogen desorption between 0.01 and 10 atm was calculated by Yates' algorithm. An alloy with x=0.35, y=0.60 (i.e., $Ti_{0.35}Zr_{0.65}Ni_{0.6}V_{1.4}$) was found to possess maximum hydrogen desorption capacity. When examined by EDAX and SEM, this alloy shows three distinguishable phases and exhibits C14 structure. The effect of substitution of Mn and Ni for V was also studied. An alloy such as $Ti_{0.35}Zr_{0.65}Ni_{1.2}V_{0.4}Mn_{0.4}$ has nearly a pure C14 structure with 89% hydrogen desorption ability. This alloy has 255mAh/g, 231mAh/g, and 210mAh/g capacities at 25mA/g, 50mA/g, and 100mA/g discharge rates, respectively. This indicates that the substitution of Mn and Ni for V not only can improve its hydrogen desorption ability but also make the alloy structure more uniform and more suitable to be an electrode material.
Order No.: JA507-015   © 1995 MRS

Microwave-Hydrothermal Processing of Metal Powders
S. Komarneni, R. Pidugu, Q.H. Li, R. Roy
(The Pennsylvania State University)

Novel microwave-hydrothermal processing has been developed by us recently for the synthesis of a wide variety of ceramic powders. Herein, we report the use of microwave-hydrothermal processing to synthesize several metal powders such as Cu, Ni, Co and Ag by reduc-
ing their corresponding metal salts or hydroxides with ethylene glycol. Metal powders have been produced extremely rapidly (minutes) by microwave catalysis. The kinetics of metal powder synthesis have been increased by at least an order of magnitude by microwave-hydrothermal processing compared to the conventional refluxing process in ethylene glycol at about 195°C.
Order No.: JA507-016   © 1995 MRS

The Cracking Resistance of Nanoscale Layers and Films
D.K. Leung, M.Y. He, A.G. Evans
(University of California-Santa Barbara)

Thin film cracking has been studied for a nanometer brittle/ductile layered system consisting of Si and Cu. Single Si films and Cu/Si/Cu trilayers were fabricated by physical vapor deposition. The films were deposited onto a ductile substrate consisting of stainless steel with a thin polyimide interlayer. Straining of the substrate induced cracking of the Si. Cracking strains $\geq 1\%$ were observed, particularly in layers ≤ 100 nm thick. The critical cracking strain was found to depend upon the Si layer thickness, as well as the thickness and elastic/plastic properties of the adjacent ductile layers. Si cracking was suppressed by the presence of adjacent Cu layers. The measured strains were compared with lower-bound critical strains for tunnel and channel cracking. Comparisons indicated that these mechanisms control the critical strain found in trilayers, because trilayer fabrication introduces edge flaws larger than the Si layer thickness. Conversely, for Si films, the measured critical strains exceed the channel cracking strain, because the flaws in these films are relatively small.
Order No.: JA507-017   © 1995 MRS

Synthetic Diamond Crystal Strength Enhancement through Annealing at 50kbar and 1500°C
S.W. Webb, W.E. Jackson
(GE Superabrasives)

High-pressure, high-temperature (HPHT) annealing of synthetic type I diamond crystals at 1200–1700°C and 50–60kbar was found to induce aggregate-nitrogen dissociation and metal coalescence, as well as heal diamond lattice dislocations. For crystals with low levels of metal inclusions, HPHT annealing was observed to increase the average compressive fracture strength of the crystals by apparently strengthening the strongest crystals of the population. Crystals with high metal-content, or otherwise of low quality, are weakened by annealing. Strengthening is believed to occur by locally stabilizing the diamond lattice by healing lattice dislocations as well as dispersing nitrogen within the lattice. A general model is presented which ties together these results with those of other researchers.
Order No.: JA507-018   © 1995 MRS

Sputtered WSi_x for Micromechanical Structures
M-L. Ger, R.B. Brown
(University of Michigan)

Tungsten silicide (WSi_x) thin films have been investigated for use as integrated circuit interconnect and self-aligned MESFET gates because of their low resistivity and thermal and chemical stability. These same characteristics make them interesting materials for prospective use in micromechanical structures. However, little information on residual stresses, elastic moduli, or other micromechanical properties has been available for refractory metal silicide thin films.

This paper presents the morphology and stress characteristics of cosputtered WSi_x thin films, including crystal structure variations and orientation-dependent stresses, as a function of the deposition pressure. The compositions of WSi_x thin films were analyzed by Rutherford backscattering spectrometry (RBS). The biaxial elastic modulus and thermal coefficient of expansion were found for the sputtered films. Stress-measurement methods and annealing are discussed. Released diaphragms of different sizes and shapes, having controlled residual stress, have been fabricated.
Order No.: JA507-019   © 1995 MRS

Mechanical Properties and Microstructure of Sputter-Deposited Nb$_5$Si$_3$/Nb Microlaminates

S.P. Rawal, G.M. Swanson, W.C. Moshier

(Martin Marietta Astronautics)

Crystalline Nb$_5$Si$_3$/Nb microlaminates were fabricated to a thickness of 20 μm by depositing the materials onto elevated temperature (750°C) substrates. Modulation wavelengths of the microlaminates were varied (λ = 40 and 200 nm) while holding their silicide volume fraction constant to assess the effect of layer thickness on the composites properties. X-ray and selected area diffraction confirmed that both the metal and silicide layers exhibited a polycrystalline structure in the as-deposited microlaminates. Nanoindentation measurements of both microlaminates indicated that calculated elastic modulus values were similar to the values obtained by the rule-of-mixtures. Nanohardness values of the microlaminates increased with decreasing wavelength in a manner described by the Hall-Petch relationship. Vickers hardness (H$_V$) measurements were also found to be a function of the modulation wavelength, decreasing from 7.32 GPa at λ = 40 nm to 3.04 GPa at λ = 200 nm. Even with a Nb volume fraction of 50%, the λ = 40 nm microlaminate and the monolithic Nb$_5$Si$_3$ film exhibited similar Vickers hardness values of 7.5 GPa. These results show the significant role of modulation wavelength on the hardness, compressive strength, and toughness characteristics of a microlaminate composite.

Order No.: JA507-020   **© 1995 MRS**

Nickel Coated Carbon Fibers Reinforced Tin-Lead Alloy Composites

C.T. Ho

(National Yun-Lin Polytechnic Institute of Technology)

Nickel is deposited over pristine, surface treated and brominated p-100 carbon fibers using cementation and electroplating techniques. The fibers are brominated by bromine vapor for 48 h and then desorbed at 200°C in air for 12 h. The anodic oxidation treatment is performed by etching fibers electrochemically in a dilute sodium electrolyte for 3 min or by immersing fibers in nitric acid for 72 hr. Electroplating coated fibers show better tensile properties than cementation coated fibers. Tin-lead alloy composites reinforced by nickel coated fibers (which are pristine, anodically oxidized and brominated) are fabricated by squeeze casting. The composites containing coated carbon fibers with bromination or surface treatment have higher tensile and shear strength than the ones containing coated pristine carbon fibers. In addition, the composite containing coated carbon fibers with bromination shows the best performance in the tensile properties.

Order No.: JA507-021   **© 1995 MRS**

Fabrication of Near-Net-Shape Al$_2$O$_3$-Fiber-Reinforced Ni$_3$Al Composites by Combustion Synthesis

W.C. Williams, G.C. Stangle

(New York State College of Ceramics at Alfred University)

In this paper, a one-step, combustion synthesis-based process for fabricating Al$_2$O$_3$ fiber-reinforced Ni$_3$Al is described. The process uses relatively low temperatures and pressures, and can be used to prepare relatively large, dense, near-net-shape articles that possess either simple or relatively complicated shapes. This process can be used to incorporate continuous, aligned fibers into the Ni$_3$Al matrix material in such a way that the fibers are not damaged either mechanically (due to relatively small applied loads during the process) or chemically (due to the very short time at which the sample remains at elevated temperatures during the process). [Chopped fibers, as well as equiaxed particles or whiskers, could also be similarly incorporated using this process.] This combustion synthesis process is a relatively simple one—requiring only relatively low temperatures and pressures, as well as relatively low-cost starting materials—which suggests that its scale-up beyond the laboratory scale would be particularly straightforward.

Order No.: JA507-022   **© 1995 MRS**

Evolution of Mechano-Chemistry and Microstructure of a Calcium Aluminate-Polymer Composite: Part I. Mixing Time Effects

M.A. Gülgün, W.M. Kriven, L.S. Tan, A.J. McHugh

(University of Illinois at Urbana-Champaign)

Paste development and evolution of microstructure, microchemistry and mechanical properties of macro-defect-free composites were investigated. Mixing torque plots from a Banbury mixer showed a "window of processibility" within which an optimum polymer-particle network structure formed. This processing window can be controlled by mixing rate and temperature. Network development during paste formation governed the flexural strength and microstructure of the cured material. Electron microscopy studies of the composites corresponding to various points along the mixing torque curve revealed a matrix formation-destruction process which was linked to the mixing activity and the mechano-chemistry of the system. Microchemical evolution in the composite was studied by EDS. These studies suggested that a combined convection and diffusion mechanism was responsible for the migration of Al^{3+} and Ca^{2+} ions into the different regions of the microstructure. Increasing concentrations of these elements in the polymer regions stiffened the matrix, leading to complete degradation on further mixing.
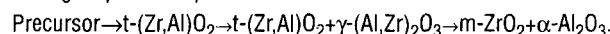
Order No.: JA507-023   **© 1995 MRS**

Phase Partitioning and Epitaxy of Zr(Al)O$_2$ Thin Films on Cubic Zirconia Substrates

P.K. Narwankar, J.S. Speck, F.F. Lange

(University of California-Santa Barbara)

Thin films of ZrO$_2$-Al$_2$O$_3$ were grown on cubic-Zr(Y)O$_2$ substrates by a liquid precursor route. Phase formation and epitaxy of these films were studied as a function of heat treatment temperature and time. The following sequence of phases was observed in these thin films:

$$\text{Precursor} \rightarrow \text{t-(Zr,Al)O}_2 \rightarrow \text{t-(Zr,Al)O}_2 + \gamma\text{-(Al,Zr)}_2\text{O}_3 \rightarrow \text{m-ZrO}_2 + \alpha\text{-Al}_2\text{O}_3.$$

Observations strongly suggest that the epitaxial process initiated before the metastable, single phase t-(Zr,Al)O$_2$ partitioned to t-(Zr,Al)O$_2$ + γ-(Al,Zr)$_2$O$_3$. Observations at 1400°C show that, after the γ to α transformation, α-Al$_2$O$_3$ grains develop an elongated, prismatic morphology and an epitaxial relation with the underlying and surrounding m-ZrO$_2$. The phase that is chemically and structurally similar to the substrate, in this case t-(Zr,Al)O$_2$, or m-ZrO$_2$, forms an epitaxial layer between the substrate and isolated, prismatic grains of heteroepitaxial α-Al$_2$O$_3$.

Order No.: JA507-024   **© 1995 MRS**

A Study of Texture in Diamond Films as Functions of Methane Concentration During Chemical Vapor Deposition Growth and Post-Growth Hydrogen Treatment

D. Ganesan, S.C. Sharma

(The University of Texas at Arlington)

We have studied effects of hydrogen on texture in diamond films grown by hot filament assisted chemical vapor deposition by utilizing x-ray diffraction (XRD). We present results for the relative intensities of the XRD peaks originating from the (111), (220) and (400) crystallographic planes as functions of CH$_4$/H$_2$ make-up during growth and post-growth H$_2$ treatment of the films. The texture of the films can be controlled by varying composition of the CH$_4$/H$_2$ mixture during growth and also by subjecting films to hydrogen treatment. The complementary characterization of these films by XRD, Raman spectroscopy, and positron annihilation techniques exemplifies a correlation between film texture, diamond contents, and density of the microvoids in the films.

Order No.: JA507-025   **© 1995 MRS**

Crystal Structure Systematics from Oxide Phase Diagrams by Contouring them with Zoltai's Tetrahedral Sharing Coefficient

B.C. Chakoumakos
(Oak Ridge National Laboratory)

For crystal structures of oxides with tetrahedral coordination polyhedra, the average number of tetrahedra participating in the sharing of a corner, i.e., Zoltai's tetrahedral sharing coefficient, provides a measure of the degree of polymerization of the tetrahedra. By contouring oxide phase diagrams with Zoltai's tetrahedral sharing coefficient, crystal structure systematics can be conveniently displayed and correlated with other physical and thermochemical properties. The advantages of this analysis are: 1) a structural map guides exploration for new compounds; 2) possible structures for existing compounds that are not known are suggested; 3) the internal consistency of the chemistry of specific compounds is tested by structural constraints; 4) the physical behavior and properties of a family of compounds in a chemical system can be correlated with the degree of polymerization of the tetrahedra; and 5) the analysis lends itself to computer programming, in that contour templates of tetrahedral sharing coefficients for different types of oxide systems can be easily determined and overlaid on traditional phase diagrams. Shortcomings to this approach are that the tetrahedral sharing coefficient does not define a unique tetrahedral anion topology, ambiguities arise if some of the oxygen atoms are not part of the tetrahedral anion, and many chemical systems contain oxides where one or more of the tetrahedral cations adopt other coordination geometries.

Order No.: JA507-026   **© 1995 MRS**

Effect of Substrates on the Crystallinity and Morphology of Sol-Gel Derived Epitaxial LiNbO$_3$ Films

K. Terabe, N. Iyi, K. Kitamura, S. Kimura
(National Institute for Research in Inorganic Materials)

Epitaxial thin films of LiNbO$_3$ were prepared by the sol-gel method on (0001)-sapphire, -LiTaO$_3$ and -5% MgO doped LiNbO$_3$ substrates. The precursor films crystallized with the highly preferred orientation on all substrates. When sapphire substrates, which have large discrepancies in the lattice constant and thermal expansion percentage with the film, were used, the resulting films showed a low crystallinity after heat-treatment at 500°C and grain growth at 650°C. On the other hand, when using LiTaO$_3$ and 5% MgO doped LiNbO$_3$ substrates, with smaller discrepancies, the formed films, after heat-treatment at 500°C, showed better crystallinity with the smooth surface.

Order No.: JA507-027   **© 1995 MRS**

Low Temperature/Low Pressure Hydrothermal Synthesis of Barium Titanate: Powder and Heteroepitaxial Thin Films

A.T. Chien, J.S. Speck, F.F. Lange, A.C. Daykin, C.G. Levi
(University of California-Santa Barbara)

Barium titanate powder and heteroepitaxial thin films were successfully produced by hydrothermal routes at ambient pressure and temperatures less than 100°C. This processing method provides a simple low temperature route for producing epitaxied barium titanate thin films on single crystal SrTiO$_3$ substrates and powders which could also be extended to other systems. A dissolution/reprecipitation growth mechanism was also proposed for the formation of barium titanate by this route using previously published aqueous stability diagrams. Repeated hydrothermal treatments improved film thickness and surface coverage at the expense of increased surface roughness.

Order No.: JA507-028   **© 1995 MRS**

Microstructures and Interdiffusions of Pt/Ti Electrodes with Respect to Annealing in the Oxygen Ambient

K.H. Park, C.Y. Kim, Y.W. Jeong, H.J. Kwon, K.Y. Kim, J.S. Lee, S.T. Kim
(Goldstar Central Research Laboratory)

The microstructural variation and the interdiffusion of Pt(80 nm)/Ti(70 nm)/SiO$_2$/Si during annealing in O$_2$ were investigated using Auger electron spectroscopy, x-ray diffraction, transmission electron microscopy, and scanning electron microscopy. While the as-deposited and 400°C annealed samples showed well-defined layer structures without any significant interfacial reaction, the degree of oxidation remarkably increased with increasing temperature above 500°C. The PtTi alloy phase with Pmma structure (AuCd type) was observed from the 500°C annealed sample. Drastic interdiffusion occurring above 600°C changed the Pt/Ti bilayer into a very entangled structure. Some TiO$_2$ phases were exposed to the ambient between Pt hillocks. In addition, a small amount of Pt-silicide was found near the TiO$_x$/SiO$_2$ interface.

Order No.: JA507-029   **© 1995 MRS**

Chemical Analyses of Stains Formed on Co-Nb-Zr MIG Heads Sliding Against Oxide and Metal Particle Magnetic Tapes

B.K. Gupta*, B. Bhushan*, Y. Zhou[+], N. Winograd[+], K. Krishnan[#]
*(*The Ohio State University, [+]The Pennsylvania State University, [#]Bio-Rad)*

The playback efficiency of metal-in-gap (MIG) inductive read-write heads in magnetic recording devices is strongly influenced by wear of the air bearing surface, metal core recession, and staining. In this study, stains were formed by sliding Co-Nb-Zr MIG tape heads against Co-γFe$_2$O$_3$ (oxide) and metal particle (MP) tapes in an accelerated mode. Optical and SEM imaging indicated that staining on a head run against the Co-γFe$_2$O$_3$ tape is thick and patchy whereas on a head run against the MP tape, staining is in the form of a uniform film. Thickness variations of stains on the metal core formed by Co-γFe$_2$O$_3$ and MP tapes, measured using atomic force microscopy (AFM), were about 30–150 nm and 20 nm, respectively. Constituents of stains were analyzed by time-of-flight secondary ion mass spectrometry (TOF-SIMS) and scanning Auger electron spectroscopy (AES), micro-Fourier transform infrared (micro-FTIR) and micro-Raman spectroscopies. Stains formed on the head run against the Co-γFe$_2$O$_3$ tape consist of organic species with trace amounts of iron and oxygen (inorganic) constituents. On the other hand, stains formed on the head run against the MP tape consist of inorganic constituents of oxidized magnetic particles from the tape. In addition to organic species and iron from tapes, stains formed by either tape also exhibit wear debris from the metal core, ferrite core, and glass region of the head itself. In the case of heads run against both tapes, most of the staining was found to be on the metal core.

Order No.: JA507-030   **© 1995 MRS**

Composites of Polypyrrole and Carbon Black. III. Chemical Synthesis and Characterization

W.A. Wampler*, K. Rajeshwar[+], R.G. Pethe[+], R.C. Hyer[+], S.C. Sharma[+]
*(*Sir Richardson Carbon Co., [+]The University of Texas at Arlington)*

A new class of molecular composites of carbon black and an electronically conducting polymer, namely polypyrrole, have been synthesized by chemically polymerizing pyrrole in an aqueous dispersion of carbon black. The carbon black content of these composites can be varied from ~5% to ~85% (by weight). The surface area and density of these composites were compared to corresponding mixtures of carbon black and polypyrrole. The influence of carbon black on the efficiency of polymerization of pyrrole is described. The effect of carbon black content on the electronic conductivity of the composite has been mapped, and compared with the corresponding behavior of a mixture of carbon black and polyvinylchloride. The influence of the parent black characteristics (porosity, void volume, surface area) on the electronic conductivity of the resultant composite has been probed by comparing the behavior of composites derived from six commercial and experimental blacks. The temperature dependence of the composites has been studied as a function of the carbon black content. Finally, the application of these new materials in an environmental remediation scenario is demonstrated for Cr(IV) as a model pollutant.

Order No.: JA507-031   **© 1995 MRS**

Removal of Residual Chromium from Aluminum Oxide by Containerless Liquid-Phase Processing

A. Biswas*, J.K.R. Weber+, P.C. Nordine+

(*Jet Propulsion Laboratory-California Institute of Technology, +Containerless Research Inc.)

Verneuil sapphire was purified of Cr^{3+} by containerless melting and processing at ca. 2550 K in argon, dry air and pure oxygen. Recovered material was examined by laser induced fluorescence and Raman spectroscopy. The Cr^{3+} fluorescence intensity decreased in processed specimens at rates proportional to the chromium concentration and $p(O_2)^{0.21}$. The initial chromium concentration was ca. 5 ppm and decreased by factors of ca. 50, 3000 and 2×10^5 after processing for 300 seconds in argon, air and oxygen, respectively. Evidence is presented that the Cr^{3+} was removed predominantly as $CrO_2(g)$ and not by conversion to other oxidation states of chromium in the condensed phase.

Order No.: JA507-032　　　　　　　© 1995 MRS

A Micromechanistic Model of the Combined Combustion Synthesis-Densification Process

Y. Zhang, G.C. Stangle

(New York State College of Ceramics at Alfred University)

A series of computer experiments has been conducted in order to study the combined combustion synthesis-densification process, in which a mechanical load is applied to a sample as it undergoes a combustion synthesis process. The current work is an extension of a theoretical model of the combustion synthesis process that was developed previously.[1,2] In this work, the appropriate constitutive equations for sample deformation have been incorporated, in order to account for the pore-volume change that may take place when the mechanical load is applied, thus densifying the sample. It was shown that the brief appearance of a liquid phase in the combustion wave front provides an important opportunity for densification when the self-propagating combustion synthesis process is conducted in conjunction with an applied mechanical load. That is, the concomitant decrease in the (local) total volume fraction of the solid phases—due to the elementary melting and dissolution processes that also occur (locally)—effectively lowered the (local) apparent yield strength of the sample, thus allowing for the compaction and densification of the sample (i.e., locally). Results indicated that the mechanical load should be applied at the instant at which the sample is ignited, in order to ensure that articles whose density is uniform throughout the sample can be fabricated. This work provided a more detailed and quantitative understanding of this unique process for preparing dense articles by the self-propagating combustion synthesis process—that is, when it is conducted in conjunction with an applied mechanical load.

Order No.: JA507-033　　　　　　　© 1995 MRS

Sintering-Viscosity Relation for Mixed-Alkali Glass Powder Compacts

K-D. Kim

(Rheinisch-Westfälische Technische Hochschule-Institut für Gesteinshüttenkunde)

The sintering of glass powder compacts was studied by dilatometer in $(25-x)Na_2O-xK_2O-75SiO_2$ glass system. The dilatometrically determined sintering temperature (T_{sin}) at constant heating rate decreases and the shrinkage at isothermal sintering increases, when Na_2O is replaced by K_2O up to the mole fraction of $K_2O/(Na_2O+K_2O)=0,5$. This is due to the decrease in viscosity and means that sintering can possibly be accelerated by introduction of mixed alkali oxides in this system. According to calculations using VFT-equation, the viscosity value at T_{sin} is almost independent of glass composition. From this result it may be suggested that the dilatometrically determined sintering begin temperature (T_{sin}) can be a characteristic point for the sintering of glass.

Order No.: JA507-034　　　　　　　© 1995 MRS